

Practical extremum-seeking control for gas-lifted oil production

Alexey Pavlov, Mark Haring and Kjetil Fjalestad

Abstract—We present a distributed extremum seeking algorithm for the problem of production optimization of multiple gas lifted wells. The algorithm is based on "synchronization" of production performance gradients for all individual wells. It mimics the manual optimization method employed by production engineers in industry. Thus due to better understanding by industrial specialists, this method may have higher chances of being accepted in the oil and gas industry compared to other data-driven optimization methods. Performance of the proposed algorithm is illustrated by simulations.

I. INTRODUCTION

Naturally flowing oil production takes place when the pressure in the oil reservoir is sufficiently high to provide economically reasonable flow rates from wells. When this is not the case, e.g. due to reservoir depletion or high density/viscosity of the produced fluid, artificial lift technologies are employed to increase the production rates. They include use of pumps and injection of gas into the well – usually referred to as gas lift. The injected gas reduces the density of the fluid column downstream the gas injection point. The corresponding reduction in the hydrostatic pressure has a positive effect on the production rate from the reservoir. However, gas injection also increases flow rate through the pipe section downstream the injection point, leading to an increased frictional pressure drop over this pipe section. This might have a negative effect on the production rate. The overall effect of the gas lift is thus a combination of the positive effect from the reduced fluid density, and the negative effect of the increased frictional pressure drop.

For relatively small gas injection rates, the positive effect is dominant. After a certain point (optimal injection rate), the negative effect becomes dominant and makes further increase of the gas injection rate unreasonable. Finding and operating at this optimal gas injection rate is one of the production optimization tasks. Of course, there are maximal and minimal limitations on the gas injection rates for each well, dictated by the limitations of the production facility.

A typical production curve that correlates the gas injection rate with the corresponding oil production rate is shown in Figure 1. The production curves are uncertain as the fluid

composition (the ratio of oil, water and gas flowing from the reservoir) changes over time. The unique optimum point and the uncertainty in the production curves makes this problem an ideal candidate for extremum seeking methods. In fact, using extremum seeking optimization for individual wells was proposed in [13], while some practical issues related to this application were addressed in [8].

A production facility consists of multiple wells and the total gas rate available for injection for all the wells is usually limited. Therefore there is a natural extension of the single well optimization problem to multiple wells. This problem fits into the framework of distributed optimization and extremum seeking control extensively studied in recent literature, see e.g. [12], [10], [2], [3], [5], [9]. It can be considered as a particular case of the optimal resource allocation problem studied in [14], [15], with the limited total available gas injection rate being the resource to be allocated between different wells. While the methods proposed in the literature provide effective solutions for generic problems, for the gas lift optimization we need to take into account specifics of practical implementation and use of automatic systems in the oil and gas industry.

Manual production optimization is done by production engineers and operators, who hold responsibility for the process. Implementation of an automatic optimization system means that certain control and optimization functions are taken away from them, while they still keep the responsibility. In this situation, people tend to be very cautious, often sceptical and reluctant to accept new automation technologies if they do not understand them, cannot easily keep track of their performance and cannot easily intervene and tune the system. From this point of view, an ideal situation is when the automation optimization system mimics an already established manual way of optimization. The operators already know it by experience and trust it.

In oil and gas production optimization, there is already a manual optimization method accepted and utilized by engineers [11]. Although in that reference the optimization problem is somewhat different, the analogy to the gas-lift optimization studied in this paper is straightforward. The method is based on a very simple fact. For the optimum allocation of gas injection rates, the gradients of the individual production curves must be equal, see, e.g. [11]. As we will show in the paper, under mild assumptions, this is a necessary and sufficient condition for optimality. In practice, the operators use the level of consensus between the gradients as a measure of optimality and steer the gas injection rates to reach this consensus [11].

In this paper we present an automatic production opti-

This work is supported by the Research Council of Norway, project number 250725, and through the Centres of Excellence function scheme, project number 223254.

A. Pavlov is with the Department of Geoscience and Petroleum, Norwegian University of Science and Technology, 7491 Trondheim, Norway alexey.pavlov@ntnu.no

M. Haring is with the Centre of Autonomous Marine Operations and Systems, Department of Engineering Cybernetics, Norwegian University of Science and Technology, 7491 Trondheim, Norway mark.haring@ntnu.no

K. Fjalestad is with Statoil Research and Technology, Porsgrunn, Norway kfja@statoil.no

mization algorithm which mimics this manual optimization method. It consists of two components: a novel gradient synchronization scheme that steers the injection rates to reach consensus between the gradients of the production curves, and a gradient estimation algorithm from [7]. Since the operators already know the concept of this solution, it is expected that it will be easier for them to accept it and use compared to other data-driven optimization methods.

The paper is organized as follows. In Section II we formalize the problem and state assumptions. Necessary and sufficient conditions for optimality based on the consensus of the gradients is presented in Section III. The same section presents a gradient synchronization algorithm. Section IV unites this algorithm with a gradient estimation method. The performance of the algorithm is illustrated in Section V. Conclusions are presented in Section VI.

II. PROBLEM DESCRIPTION

We consider a production system with N individual wells with gas lift. For each well i , oil production rate q_i as a function of the gas injection rate u_i is determined by the production curve

$$q_i = f_i(u_i), \quad (1)$$

with a typical form as in Figure 1. The gas injection rates are subject to constraints

$$0 \leq u_i^{\min} \leq u_i \leq u_i^{\max}, \quad i = 1, \dots, N. \quad (2)$$

The total gas injection rate is subject to the constraint

$$\sum_{i=1}^N u_i \leq U^{\max}. \quad (3)$$

The optimization problem is to maximize the total production rate from all the wells

$$\sum_{i=1}^N f_i(u_i) \rightarrow \max \quad (4)$$

subject to constraints (2), (3).

We assume that the functions f_i are C^2 and that they are strictly concave, i.e.

$$\frac{d^2 f_i}{du_i^2}(u_i) < 0, \quad \forall u_i \in [u_i^{\min}, u_i^{\max}], \quad i = 1, \dots, N. \quad (5)$$

Under these assumptions, the optimization problem (2), (3), (4) has a unique solution.

Before solving this problem, we modify its formulation in the following way. We first introduce the fictitious input u_{N+1} which denotes the available gas rate not injected into the wells: $u_{N+1} = U^{\max} - \sum_{i=1}^N u_i$. It must satisfy the constraint $0 = u_{N+1}^{\min} \leq u_{N+1} \leq u_{N+1}^{\max} = U^{\max}$.¹ The corresponding fictitious function $f_{N+1}(u_{N+1})$ is set to zero.

¹Note that since $u_i \geq 0$ for $i = 1, \dots, N$, then the inequality with u_{N+1}^{\max} is always satisfied and thus becomes obsolete. However, for the sake of uniformity of the presentation, we will keep this inequality.

Then the optimization problem (2), (3), (4) is equivalent to the problem

$$\sum_{i=1}^{N+1} f(u_i) \rightarrow \max \quad (6)$$

under the constraints

$$\sum_{i=1}^{N+1} u_i = U^{\max}, \quad (7)$$

$$u_i^{\min} \leq u_i \leq u_i^{\max}, \quad i = 1, \dots, N+1. \quad (8)$$

The reason for the modification from the inequality constraint in (3) to equality constraint in (7) will be explained below.

Further, we modify the problem formulation to handle the case when the optimum can lie on the boundary of the constraints (8). We augment the functions f_i with logarithmic barrier functions:

$$\hat{f}_i(u_i) = \begin{cases} f_i(u_i) + \mu \ln(u_i - u_i^{\min}) \\ \quad + \mu \ln(u_i^{\max} - u_i), & \text{if } u_i \in (u_i^{\min}, u_i^{\max}), \\ -\infty, & \text{otherwise,} \end{cases} \quad (9)$$

for $i \in \{1, 2, \dots, N+1\}$, where $\mu > 0$ is a tuning constant, and rewrite the optimization problem in a compact form:

$$Q(\mathbf{u}) = \sum_{i=1}^{N+1} \hat{f}_i(u_i) \rightarrow \max, \quad (10)$$

over the domain

$$\mathcal{U} := \{\mathbf{u} \mid u_i \in (u_i^{\min}, u_i^{\max}), \quad i = 1, \dots, N+1\} \quad (11)$$

and subject to the equality constraint

$$\mathbf{1}^T \cdot \mathbf{u} = U^{\max}, \quad (12)$$

where $\mathbf{1} = (1, \dots, 1)^T$ and $\mathbf{u} = (u_1, \dots, u_{N+1})^T$.

Since the logarithmic functions are strictly concave and the functions f_i are concave, then the functions $\hat{f}_i(u_i)$ are strictly concave on the set (u_i^{\min}, u_i^{\max}) . Moreover, due to the barrier functions, $\hat{f}_i(u_i) \rightarrow -\infty$ as $u_i \rightarrow u_i^{\min}$ or $u_i \rightarrow u_i^{\max}$. Thus the optimization problem (10) - (12) has a unique optimum point $\mathbf{u}^* \in \mathcal{U}$.

By choosing parameter μ small enough, the solution to the optimization problem (10) - (12) can be chosen arbitrarily close to the optimum of the original optimization problem (2), (3), (4). In the sequel we assume that the parameter μ is chosen and we will focus on solving the modified optimization problem (10) - (12).

III. SYNCHRONIZATION-BASED OPTIMIZER

First, we derive a simple technical result that constitutes a foundation for the optimizer design.

Lemma 1: Point $\mathbf{u}^* \in \mathcal{U}$ is a solution to the optimization problem (10) - (12) if and only if

$$\frac{\partial \hat{f}_i}{\partial u_i}(u_i^*) = \frac{\partial \hat{f}_j}{\partial u_j}(u_j^*), \quad \forall i, j = 1, \dots, N+1. \quad (13)$$

Proof: We parametrize the hyperplane (12), by the equation $u_{N+1} = U^{max} - \sum_{i=1}^N u_i$. Substituting this parametrization in the definition of $Q(\mathbf{u})$, we obtain

$$\begin{aligned} Q(\mathbf{u})|_{\mathbf{1}^T \cdot \mathbf{u} = U^{max}} &= \sum_{i=1}^N \hat{f}_i(u_i) + \hat{f}_{N+1}(U^{max} - \sum_{i=1}^N u_i) \\ &=: \tilde{Q}(u_1, \dots, u_N). \end{aligned} \quad (14)$$

Since $Q(\mathbf{u})$ is strictly concave, $\tilde{Q}(u_1, \dots, u_N)$ is strictly concave as well. Thus the necessary and sufficient condition for its optimal point is $\partial \tilde{Q} / \partial u_i(\mathbf{u}^*) = 0$ for $i = 1, \dots, N$. Substituting this condition into (14), we obtain

$$\frac{\partial \hat{f}_i}{\partial u_i}(u_i^*) - \frac{\partial \hat{f}_{N+1}}{\partial u_{N+1}}(u_{N+1}^*) = 0, \quad \forall i = 1, \dots, N. \quad (15)$$

This, in turn, is equivalent to (13). \square

Corollary 1: There is only one point $\mathbf{u}^* \in \mathcal{U}$ satisfying (13) and (12) and this point is the solution to the optimization problem (10) - (12).

Based on this corollary, we construct the following update law for \mathbf{u} :

$$\dot{u}_i = \sum_{j \neq i} \gamma_{i,j} \left(\frac{\partial \hat{f}_i}{\partial u_i}(u_i) - \frac{\partial \hat{f}_j}{\partial u_j}(u_j) \right), \quad (16)$$

for $i = 1, \dots, N+1$, where $\gamma_{i,j} = \gamma_{j,i} \geq 0$ are synchronization gains. The right hand side of (16) equals zero when all the gradients are equal to each other ("synchronized"). When this is not the case, (16) will steer the components of \mathbf{u} towards gradients synchronization.

To show this, let us rewrite the update law (16) in the following compact form:

$$\dot{\mathbf{u}} = \Gamma \nabla Q(\mathbf{u}), \quad (17)$$

where

$\Gamma =$

$$\begin{bmatrix} \sum_{j \neq 1} \gamma_{1,j} & -\gamma_{1,2} & \cdots & -\gamma_{1,N+1} \\ -\gamma_{2,1} & \sum_{j \neq 2} \gamma_{2,j} & \cdots & -\gamma_{2,N+1} \\ -\gamma_{3,1} & -\gamma_{3,2} & \ddots & \vdots \\ \vdots & \vdots & \ddots & -\gamma_{N,N+1} \\ -\gamma_{N+1,1} & -\gamma_{N+1,2} & \cdots & \sum_{j \neq N+1} \gamma_{N+1,j} \end{bmatrix}.$$

Theorem 1: Under the assumptions on the function $Q(\mathbf{u})$ from Section II, if $\text{rank} \Gamma = N$, then for any initial condition $\mathbf{u}(0) \in \mathcal{U}$ satisfying (12), the solution $\mathbf{u}(t)$ will satisfy (12) for all $t \geq 0$ and

$$\mathbf{u}(t) \rightarrow \mathbf{u}^*, \text{ as } t \rightarrow +\infty \quad (18)$$

where \mathbf{u}^* is the unique optimal solution to the optimization problem (10) - (12).

Proof: Due to its structure, the matrix $\Gamma = \Gamma^T$ is positive semidefinite [17], and satisfies

$$\mathbf{1}^T \Gamma = 0. \quad (19)$$

From (19) and (17), we obtain

$$\frac{d}{dt} \mathbf{1}^T \mathbf{u}(t) = \mathbf{1}^T \Gamma \nabla Q(\mathbf{u}) \equiv 0. \quad (20)$$

Thus if $\mathbf{1}^T \mathbf{u}(0) = U^{max}$, then $\mathbf{1}^T \mathbf{u}(t) = U^{max}$ (i.e. (12) is satisfied) for all $t \geq 0$.

To prove (18), consider the storage function $V(\mathbf{u}) = Q(\mathbf{u}^*) - Q(\mathbf{u})$. Then

$$\frac{d}{dt} V(\mathbf{u}(t)) = -\nabla Q^T(\mathbf{u}) \Gamma \nabla Q(\mathbf{u}) \leq 0 \quad \forall \mathbf{u} \in \mathcal{U}. \quad (21)$$

Therefore $V(\mathbf{u}(t)) \leq V(\mathbf{u}(0))$ for all $t \geq 0$. Hence, the set $\Omega := \{\mathbf{u} \mid V(\mathbf{u}) \leq V(\mathbf{u}(0))\}$ is a positively invariant, compact subset of \mathcal{U} . Since $\text{rank} \Gamma = N$, (for the $(N+1) \times (N+1)$ matrix), and since $\mathbf{1}^T \Gamma = 0$ and $\Gamma \mathbf{1} = 0$, then the set $\mathcal{S} := \{\mathbf{u} \mid \dot{V}(\mathbf{u}) = 0\}$ consists of points where $\nabla Q(\mathbf{u}) = \alpha(\mathbf{u}) \mathbf{1}$, for some scalar $\alpha(\mathbf{u})$, i.e. condition (13) is satisfied. According to LaSalle's invariance principle, $\mathbf{u}(t)$ converges to the largest invariant subset of \mathcal{S} . By the corollary to Lemma 1, under the assumptions on the function $Q(\mathbf{u})$ from Section II, there is only one point satisfying both (13) and (12) and this point is the optimum \mathbf{u}^* . This proves (18). \square

Remark 1. The matrix Γ determines the structure for the synchronization of the gradients in the form of a graph: node j affects the update dynamics of node i (there is an edge between them) if $\gamma_{i,j} > 0$. The requirement $\text{rank} \Gamma = N$ is satisfied if this graph is connected, i.e. any two nodes can be connected by a path of edges with nonzero gains $\gamma_{i,j}$.

Remark 2. The requirement that $\mathbf{u}(0)$ is initiated at the hyperplane $\mathbf{1}^T \cdot \mathbf{u} = U^{max}$ can always be satisfied by the choice of the fictitious variable u_{N+1} .

Remark 3. It can also be shown that in the reduced coordinates u_1, \dots, u_N , the convergence to the optimal u_1^*, \dots, u_N^* is exponential. This results in certain robustness needed when the gradients in (16) are substituted with their estimates, as described in the next section.

IV. EXTREMUM-SEEKING METHOD

Because the functions f_i are unknown, the gradients of the augmented functions \hat{f}_i in (9) cannot be used by the controller to solve the optimization problem. We estimate the gradients using a perturbation-based approach that is common to extremum-seeking control [1], [16]. Consider the following coordinate transformation:

$$u_i(t) = \bar{u}_i(t) + \alpha \omega_i(t), \quad \omega_i(t) = \sin \left(\eta t + \frac{2\pi(i-1)}{N} \right) \quad (22)$$

for $i \in \{1, 2, \dots, N\}$, where \bar{u}_i is the nominal part of the input and $\alpha \omega_i$ is a perturbation with amplitude $\alpha > 0$ and angular frequency $\eta > 0$. The phase of the perturbations is chosen such that

$$\sum_{i=1}^N \alpha \omega_i(t) = 0 \quad \Rightarrow \quad \sum_{i=1}^N u_i(t) = \sum_{i=1}^N \bar{u}_i(t) \quad (23)$$

for all $t \in \mathbb{R}$. This implies that the total gas injection rate is not affected by the perturbation signals. This is a

practically important property, since perturbations on the total injection rate can cause undesirable negative effects for the overall production/processing system. We slightly modify the augmented functions in (9) such that \mathbf{u} remains in the set \mathcal{U} if $\bar{\mathbf{u}} = [\bar{u}_1, \bar{u}_2, \dots, \bar{u}_N]^T$ remains in the set

$$\mathcal{U}_\alpha = \left\{ \bar{\mathbf{u}} \in \mathbb{R}^N : u_i^{\min} + \alpha < \bar{u}_i < u_i^{\max} - \alpha, \right. \\ \left. \forall i \in \{1, 2, \dots, N+1\} \right\}. \quad (24)$$

We note that, if the set \mathcal{U} is nonempty, the set \mathcal{U}_α is nonempty for sufficiently small $\alpha > 0$. The modified augmented functions are given by

$$\bar{f}_i(\bar{u}_i) = \begin{cases} f_i(\bar{u}_i) + \mu \ln(\bar{u}_i - u_i^{\min} - \alpha) \\ \quad + \mu \ln(u_i^{\max} - \alpha - \bar{u}_i), \\ \quad \text{if } \bar{u}_i \in (u_i^{\min} + \alpha, u_i^{\max} - \alpha), \\ -\infty, \quad \text{otherwise,} \end{cases} \quad (25)$$

for $i \in \{1, 2, \dots, N\}$ and

$$\bar{f}_{N+1}(\bar{u}_{N+1}) = \hat{f}_{N+1}(\bar{u}_{N+1}). \quad (26)$$

Due to these modifications, we aim at finding the solution of the optimization problem

$$\bar{Q}(\bar{\mathbf{u}}) := \sum_{i=1}^{N+1} \bar{f}_i(\bar{u}_i) \rightarrow \max \quad (27)$$

over the domain $\bar{\mathbf{u}} \in \mathcal{U}_\alpha$ and subject to the constraint $\mathbf{1}^T \cdot \bar{\mathbf{u}} = U^{\max}$. We note, however, that the solution of the optimization problem (27) can be made arbitrarily close to the solution of the optimization problem (10) - (12) by choosing a sufficiently small value of $\alpha > 0$. To find an approximate solution of the optimization problem (27), we estimate the gradients of the augmented functions \bar{f}_i in (25). Contrary to the constrained extremum-seeking method in [4] which estimates the gradients of the augmented functions directly, we estimate the gradients of the functions f_i and use these gradient estimates to approximate the gradient of the modified augmented functions \bar{f}_i ; the known contributions of the logarithmic barrier functions are added to the estimated gradients of f_i to obtain the gradients of \bar{f}_i . This has the advantage that the logarithmic barrier functions prevent the nominal input $\bar{\mathbf{u}}$ from leaving the set \mathcal{U}_α even if the gradient estimates are bad. For each $i \in \{1, 2, \dots, N\}$, we apply the observer from [7] to estimate the gradient of the function f_i . The observer estimates the vector

$$\mathbf{m}_i(t) = \begin{bmatrix} f_i(\bar{u}_i(t)) \\ \alpha \frac{df_i}{du_i}(\bar{u}_i(t)) \end{bmatrix}. \quad (28)$$

The time derivative of this vector is given by

$$\dot{\mathbf{m}}_i(t) = \mathbf{A}_i(t)\mathbf{m}_i(t) + \mathbf{w}_i(t), \quad \mathbf{A}_i(t) = \begin{bmatrix} 0 & \dot{\bar{u}}_i(t) \\ 0 & \alpha \end{bmatrix},$$

with $\mathbf{w}_i(t) = \mathcal{O}(\alpha \dot{\bar{u}}_i(t))$ as $\alpha \dot{\bar{u}}_i(t) \rightarrow 0$, where \mathcal{O} is the Big O notation. From Taylor's theorem and (22), it follows that

$$y_i(t) = f_i(u_i(t)) = f_i(\bar{u}_i(t)) + \alpha \omega_i(t) \frac{df_i}{du_i}(\bar{u}_i(t)) + v_i(t)$$

where $v_i(t) = \mathcal{O}(\alpha^2)$ as $\alpha \rightarrow 0$ is the remainder of the Taylor series expansion around $\bar{u}_i(t)$. Using the definition of the vector \mathbf{m}_i , this equality can be written as

$$y_i(t) = \mathbf{C}_i(t)\mathbf{m}_i(t) + v_i(t), \quad \mathbf{C}_i(t) = [1 \quad \omega_i(t)]. \quad (29)$$

The corresponding observer is given by

$$\dot{\hat{\mathbf{m}}}_i(t) = \mathbf{A}_i(t)\hat{\mathbf{m}}_i(t) + \lambda \mathbf{P}_i(t)\mathbf{C}_i^T(t)(y_i(t) - \mathbf{C}_i(t)\hat{\mathbf{m}}_i(t)) \\ \dot{\mathbf{P}}_i(t) = \lambda \mathbf{P}_i(t) + \mathbf{A}_i(t)\mathbf{P}_i(t) + \mathbf{P}_i(t)\mathbf{A}_i^T(t), \\ - \lambda \mathbf{P}_i(t)\mathbf{C}_i^T(t)\mathbf{C}_i(t)\mathbf{P}_i(t), \quad (30)$$

where \mathbf{P}_i is a symmetric positive-definite matrix and $\lambda > 0$ is a tuning parameter. Noting that $\hat{\mathbf{m}}_i$ is an estimate of the vector \mathbf{m}_i in (28), we obtain that

$$\bar{g}_i(t) = \mathbf{D}\hat{\mathbf{m}}_i(t) + \frac{\alpha\mu}{\bar{u}_i(t) - u_i^{\min} - \alpha} - \frac{\alpha\mu}{u_i^{\max} - \alpha - \bar{u}_i(t)} \quad (31)$$

for $i \in \{1, 2, \dots, N\}$, with $\mathbf{D} = [0, 1]$, is an estimate for the gradient of the function \bar{f}_i in (25) scaled by the perturbation amplitude α . For notational convenience, we define

$$\bar{g}_{N+1}(t) = \frac{\alpha\mu}{\bar{u}_{N+1}(t)}, \quad (32)$$

which is the product of the gradient of the function \bar{f}_{N+1} in (26) and the perturbation amplitude α .

Similar to (16) in Section III, we use the optimizing control law

$$\dot{\bar{u}}_i(t) = \nu \sum_{j \neq i} \gamma_{i,j} (\bar{g}_i(t) - \bar{g}_j(t)) \quad (33)$$

to drive the nominal input $\bar{\mathbf{u}}$ to the solution of the optimization problem (27), where $\nu > 0$ is a tuning parameter. Note that, contrary to the control law (16), scaled estimates of the gradients of the functions \bar{f}_i are used instead of the real gradients.

A. Tuning of the controller parameters

The accuracy of the estimates \bar{g}_i in (31) of the gradients of the functions \bar{f}_i depends to a large extent on the tuning of the extremum-seeking controller. There are four parameters to tune: the perturbation amplitude α in (22); the perturbation frequency η in (22); the tuning parameter λ of the observers in (30); and the tuning parameter ν of the dynamic optimizer in (33). As mentioned previously, the perturbation amplitude should be chosen sufficiently small to ensure that solution of the optimization problem (27) is sufficiently close to the solution of the optimization problem (10) - (12). However, in practice, the perturbation amplitude is required to be sufficiently large to ensure that the gradient estimates are not driven by disturbances such as measurement noise. Especially disturbances in the same frequency range as the perturbation frequency are harmful in this regard; see [6],

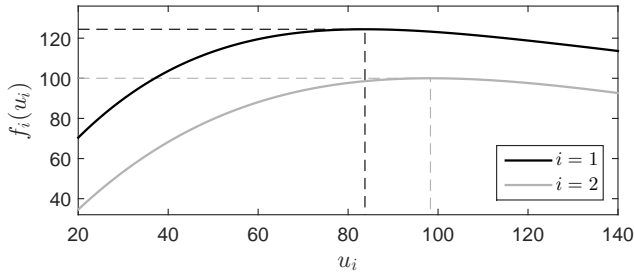


Fig. 1. Well-performance curves.

[16]. To obtain accurate gradient estimates with the observers in (30), the remaining tuning parameters should be chosen such that extremum-seeking controller roughly exhibits three time scales [6], [7]:

- fast – the perturbations;
- medium – the observers;
- slow – the dynamic optimizer.

For any fixed value of $\alpha > 0$, this can be achieved by choosing the tuning parameters η , λ and ν such that $\nu \ll \lambda \ll \eta$. Detailed convergence analysis is given in [7]. Without system dynamics, as we assume in this work, the perturbation frequency η can be chosen arbitrarily large. In practical applications, the perturbation frequency should be chosen sufficiently low such that, after initial transients, the output of the systems remains close to the steady-state output of the systems despite system dynamics.

V. SIMULATION EXAMPLE

Consider two wells with gas lift. Let the gas injection rates of the two wells be given by u_1 and u_2 , respectively. The relation between the gas injections rates and the corresponding oil rates q_1 and q_2 is given by the well-performance curves

$$\begin{aligned} f_1(u_1) &= -3.9 \times 10^{-7} u_1^4 + 2.1 \times 10^{-4} u_1^3 \\ &\quad - 0.043 u_1^2 + 3.7 u_1 + 12, \\ f_2(u_2) &= -1.3 \times 10^{-7} u_2^4 + 1 \times 10^{-4} u_2^3 \\ &\quad - 0.028 u_2^2 + 3.1 u_2 - 17. \end{aligned} \quad (34)$$

The well-performance curves are visualized in Fig. 1, where the maximum of the curves at $(u_1^*, u_2^*) \approx (83.7, 98.3)$ is indicated by dashed lines. The gas injection rates are bounded by the lower limits $u_1^{\min} = u_2^{\min} = 20$ and the upper limits $u_1^{\max} = u_2^{\max} = 140$. We consider two scenarios: for the first scenario, the maximal combined gas injection rate is bounded by $U^{\max} = 200$; for the second scenario, it is bounded by $U^{\max} = 160$. We use the extremum-seeking control method in Section IV to maximize the combined oil rate of the two wells. The tuning parameters of the extremum-seeking controller are set to $\alpha = 2$, $\eta = 1$, $\lambda = 0.5$, $\gamma_{12} = \gamma_{13} = \gamma_{21} = 1$, $\gamma_{23} = 0$ and $\nu = 1$. In addition, we set $\mu = 10^{-3}$. Simulation results for $u_1(0) = 100$ and $u_2(0) = 40$ are presented in Figs. 2-7.

The trajectory of the gas injection rates u_1 and u_2 for $U^{\max} = 200$ is depicted in Fig. 2. The solid black contour in Fig. 2 represents the boundary of the feasible region; the

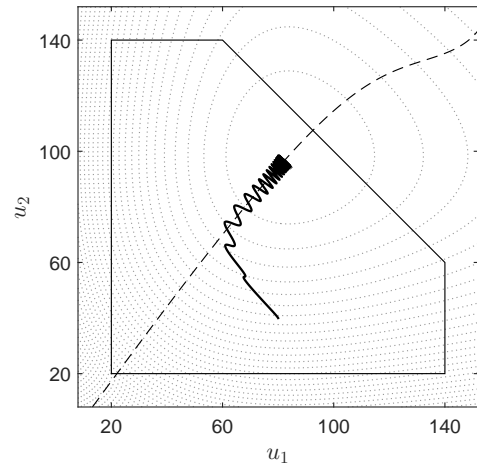


Fig. 2. Trajectory of the gas injection rates u_1 and u_2 for $U^{\max} = 200$.

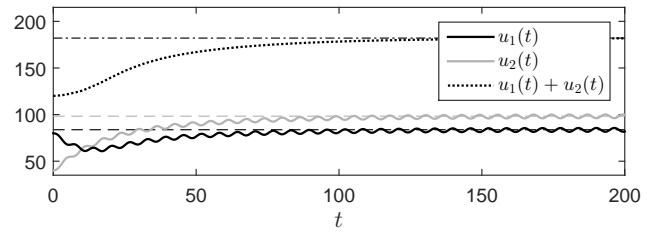


Fig. 3. Gas rates u_1 , u_2 and their sum vs. time t for $U^{\max} = 200$.

dashed black line in Fig. 2 is the line for which $\frac{\partial f_1}{\partial u_1}(u_1) = \frac{\partial f_2}{\partial u_2}(u_2)$. We observe in Fig. 2 that using the synchronization-based control law in Section III, the trajectory of the gas injection rates converges to the line $\frac{\partial f_1}{\partial u_1}(u_1) = \frac{\partial f_2}{\partial u_2}(u_2)$ before it converges to a neighborhood of the optimum.

The corresponding time signals of the gas injection rates are depicted in Fig. 3. The values of the gas injection rates converge to a neighborhood of the optimal values $u_1^* \approx 83.7$ and $u_2^* \approx 98.3$ indicated by the dashed lines in Fig. 3. It is easy to see in Fig. 3 that the perturbations in the gas injection rate signals have the same amplitude and frequency, but an opposite phase, as defined in (22). As the gas injection rates converge to a neighborhood of the optimum, it is shown in Fig. 5 that the well performance converges to a value that is very close to its optimal value of $Q(\mathbf{u}^*) \approx 224.5$ indicated by the dashed line.

In Figs. 5-7, we see similar results for $U^{\max} = 160$ as for $U^{\max} = 200$ in Figs. 2-4. However, contrary to the scenario $U^{\max} = 200$, the constraint $u_1 + u_2 \leq U^{\max}$ is active at the optimum for $U^{\max} = 160$. This can be clearly observed in Fig. 5, where the trajectory of the gas injection rates is held back by the diagonal line of the solid black contour representing the constraint $u_1 + u_2 \leq U^{\max}$. The constrained optimum $Q(\mathbf{u}^*) \approx 222.7$ is achieved for gas injection rates $u_1^* \approx 73.5$ and $u_2^* \approx 86.5$. Figs. 6 and 7 display that convergence to a small neighborhood of these values is achieved.

Notice that in both simulations, due to a deliberate choice of phase shifts in the dither signals, the total gas injection

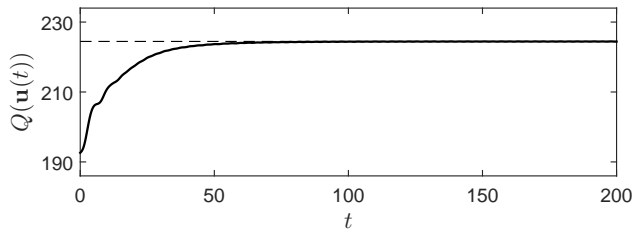


Fig. 4. Total oil production rate $Q(\mathbf{u})$ vs. time t for $U^{\max} = 200$.

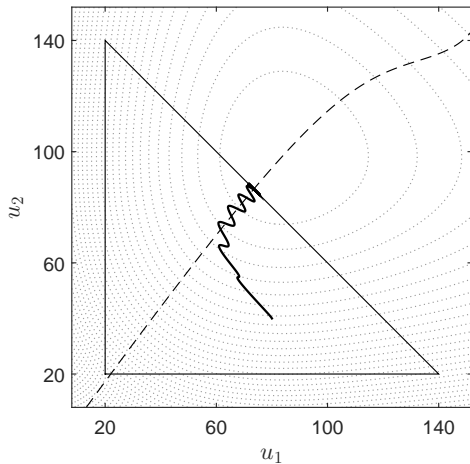


Fig. 5. Trajectory of the gas injection rates u_1 and u_2 towards the optimum at $(u_1^*, u_2^*) \approx (73.5, 86.5)$ for $U^{\max} = 160$.

rate and the total oil production rate corresponding to all wells are not subject to the variations due to dither signal. This is especially important since topside facilities can be sensitive to frequent changes of the total injected gas rates and produced oil rates. This is another practical benefit of the proposed method.

VI. CONCLUSIONS AND FUTURE WORK

In this paper we have presented a distributed extremum seeking algorithm for the optimal resource allocation problem, with the main motivation for the study being production optimization for multiple gas lifted wells. The proposed solution is based on a novel extremum seeking scheme utilizing synchronization of the performance functions' gradients as a measure of optimality. This scheme is then united with a gradient estimation method. The overall solution has demonstrated good performance in simulations. More importantly, it automatically mimics the manual optimization methods employed by operators and production engineers in the oil and gas industry. Thus due to better understanding of this method by industrial specialists, it has higher chances of being accepted and used for production optimization in the oil and gas industry compared to other data-driven optimization methods. Future work will be focused on practical aspects related to implementation, tuning and running of the proposed solution on a production platform.

REFERENCES

[1] K. B. Ariyur and M. Krstić. *Real-time optimization by extremum-seeking control*. Wiley-Interscience, Hoboken, NJ, 2003.

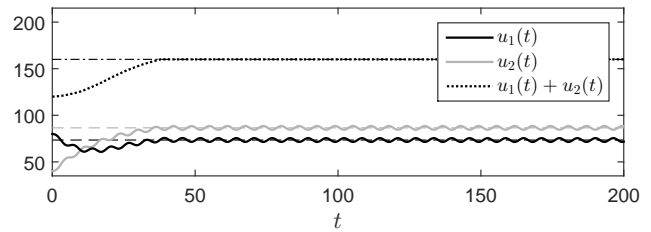


Fig. 6. Gas rates u_1 , u_2 and their sum vs. time t for $U^{\max} = 160$.

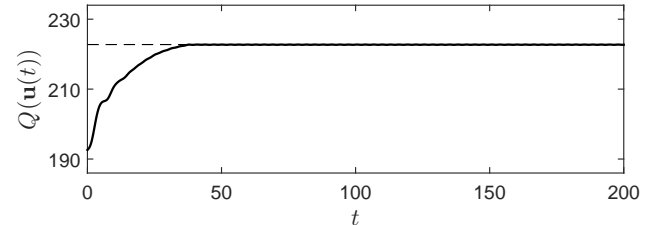


Fig. 7. Total oil production rate $Q(\mathbf{u})$ vs. time t for $U^{\max} = 160$.

- [2] S. Dougherty and M. Guay. Extremum-seeking control of distributed systems using consensus estimation. In *Proceedings of the 53rd IEEE Conference on Decision and Control*, Los Angeles, CA, USA, 2014.
- [3] S. Dougherty and M. Guay. An extremum-seeking controller for distributed optimization over sensor networks. *IEEE Transactions on Automatic Control*, 62(2):928–933, 2015.
- [4] M. Guay, E. Moshksar, and D. Dochain. A constrained extremum-seeking control approach. *International Journal of Robust and Nonlinear Control*, 25:3132–3153, 2015.
- [5] M. Guay, I. Vandermeulen, S. Dougherty, and P.J. Mclellan. Distributed extremum-seeking control over networks of dynamic agents. In *Proc. 2015 American Control Conference*, 2015.
- [6] M. Haring and T. A. Johansen. Asymptotic stability of perturbation-based extremum-seeking control for nonlinear plants. *IEEE Transactions on Automatic Control*, 2016. Accepted for publication.
- [7] M. A. M. Haring. *Extremum-seeking control: convergence improvements and asymptotic stability*. PhD thesis, NTNU, 2016.
- [8] D. Krishnamoorthy, A. Pavlov, and Q. Li. Robust extremum seeking control with application to gas lifted oil wells. In *Proceedings of the 12th IFAC Workshop on Adaptation and Learning in Control and Signal Processing*, Eindhoven, The Netherlands, 2016.
- [9] K. Kvaternik and L. Pavel. An analytic framework for decentralized extremum seeking control. In *Proceedings of the 2012 American Control Conference*, Montreal, Canada, 2012.
- [10] P. Lin, W. Ren, and J.A. Farrell. Distributed continuous-time optimization: Nonuniform gradient gains, finite-time convergence, and convex constraint set. *IEEE Transactions on Automatic Control*, 62(5), 2017.
- [11] A. Mjaavatten, R. Aasheim, S. Saelid, and Groning O. A model for gas coning and rate-dependent gas/oil ratio in an oil-rim reservoir. In *Proceedings of SPE Russian Oil and Gas Technical Conference and Exhibition, SPE102390*, Moscow, Russia, 2006.
- [12] A. Nedic, A. Ozdaglar, and A.P. Parrilo. Constrained consensus and optimization in multi-agent networks. *IEEE Transactions on Automatic Control*, 55(4):922–938, 2010.
- [13] A. Peixoto, D. Pereira-Dias, A. Xaud, and A. Secchi. Modelling and extremum seeking control of gas lifted oil wells. In *Proceedings of the 2nd IFAC Workshop on Automatic Control in Offshore Oil and Gas Production*, Florianopolis, Brazil, 2015.
- [14] J. Poveda and N. Quijano. Distributed extremum seeking for real-time resource allocation. In *Proceedings of the 2013 American Control Conference (ACC)*, Washington DC, USA, 2013.
- [15] J. Poveda and N. Quijano. Shahshahani gradient-like extremum seeking. *Automatica*, 58:51–59, 2015.
- [16] Y. Tan, W. H. Moase, C. Manzie, D. Nešić, and I. M. Y. Mareels. Extremum seeking from 1922 to 2010. In *Proceedings of the 29th Chinese Control Conference*, Beijing, China, July 29–31, 2010.
- [17] R.S. Varga. *Gerschgorin and His Circles*. Springer-Verlag, 2004.